

The above discussion has assumed that the grating is used in a diffraction configuration, as in a cross arrangement of a beam splitter, high reflectivity region, and shift. If the grating is used in a filter configuration, also problems due to the finite conductivity of the metallic coating of the grating have been neglected, so the analysis applies best at wavelengths longer than 1  $\mu\text{m}$ . It is worth noting that the reflectivity for TE becomes very high ( $\lambda < \lambda_c$ ) but for a pulsed laser an even more serious difficulty may be encountered. For a circular, however, the cavity generally has Brewster-angle elements oriented to pass  $E_{\perp}$  which would produce for much higher reflection with  $E_{\parallel}$ .

As will be seen, the slow-wave grating offers separate features not other than first-order wavelengths such that  $\frac{1}{2}d \leq \lambda \leq 2d$ . For an example of a 400-groove/mm with  $\lambda_c = 2.6 \mu\text{m}$  and  $\lambda_s = 3.3 \mu\text{m}$ , this implies propagation of only the higher order harmonics. The surface impedance is between 200 lines/mm and 600 lines/mm. If  $d$  is selected so that  $\lambda_c = \lambda_s$  and  $\lambda_s = \lambda_l$ , the grating becomes

$$d = \frac{1}{2}(\lambda_s^2 + \lambda_l^2)^{1/2},$$

which is about 400 lines/mm. Such a choice would give the highest reflectivity at the ends of the present tuning range where the gain is the lowest, and a higher output coupling in the middle where the gain is higher.

In Fig. 2 the performance of several rulings is plotted. Two of the rulings have  $d^{-1} = 420$  grooves/mm and are blazed at  $2.15 \mu\text{m}$  which puts the second peak at about  $4.25 \mu\text{m}$ . These parameters are close to the condition for minimum threshold deduced above, but provide a somewhat broader tuning range. Because of the groove shape, one ruling gives an output coupling of about 1.5%, while the other one is nearly 12%. The other case in Fig. 2 shows a 400-groove/mm grating selected for high output power operation so that  $\lambda_s < \lambda_c$  and  $\lambda_c > \lambda_l$ , which produces a peak output coupling of about 22%.

The F-center laser has been made to function with each of these gratings, and the thresholds and output powers fit the external reflectivity measurements given in Fig. 2. For example, in the cavity described by German,<sup>2</sup> the grating in Fig. 2 represented by the closed circles produced lasing for all three crystals with external pump powers of less than 100 mW, and the entire tuning range could be covered with a 1-W pump laser. The measured reflectivity of this grating was  $\geq 95\%$  from  $2.0 \mu\text{m}$  to  $4.5 \mu\text{m}$  and clearly fulfills the design objective of a broadband high-reflectivity tuner.

## References

1. E. G. Loewen, M. Neviere, and D. Maystre, *Appl. Opt.* **16**, 2711 (1977).
2. K. R. German, *Opt. Lett.* **4**, 68 (1979).

## Comparison of Fourier and laser spectroscopy in the far-infrared-submillimeter range

S. Perkowitz, R. L. Henry, and D. B. Tanner.

S. Perkowitz is with Emory University, Physics Department, Atlanta, Georgia 30322; the other authors are with Ohio State University, Physics Department, Columbus, Ohio 43210.

Received 4 May 1979.

0003-6935/79/142349-03\$00.50/0.

© 1979 Optical Society of America.

Successful spectroscopy in the submillimeter-far-infrared (far-IR) region is a difficult task and unconventional

methods have commonly been employed in this frequency range.<sup>1</sup> Fourier spectroscopy replaced the then-conventional grating techniques some 15 years ago and still dominates the field. During the transition from grating to Fourier spectroscopy the new method had to prove itself, and several comparison and performance studies were published.<sup>2-7</sup> Recently a new device, the optically pumped far-IR laser, has shown promise as a high-power spectral source. Now, careful comparisons between the established Fourier technique and the new laser spectroscopy are called for. In this Letter we compare state-of-the-art Fourier spectrometers with a recently built laser system by describing measurements made on the same sample, a thin film of the metallic superconductor  $\text{V}_3\text{Si}$  deposited on a sapphire substrate. The very low transmission of this sample provided a demanding test of spectral performance, and the comparison clearly shows the strengths and weaknesses of the two methods.

Two Fourier spectrometers, located at the Ohio State University, were employed in these measurements. A lamellar grating interferometer<sup>8</sup> covered  $6\text{--}30 \text{ cm}^{-1}$ , while a Michelson interferometer<sup>9</sup> was used over  $50\text{--}200 \text{ cm}^{-1}$ . These instruments have effective numerical apertures of  $f/1.6$ , employ 1.27-cm-diameter light-pipe optics, and use the same type of mercury arc lamp source (General Electric UA-3). In the  $6\text{--}30\text{-cm}^{-1}$  region this lamp has an apparent color temperature<sup>6</sup> of 4000 K and emits into the aperture  $\sim 5 \times 10^{-6} \text{ W}$  of far-IR power. In the  $50\text{--}200\text{-cm}^{-1}$  region the color temperature is lower, approximately 1000 K, and the total power delivered is  $\sim 2 \times 10^{-4} \text{ W}$ .

In the lamellar grating interferometer, beam division and interferometric modulation are achieved by two sets of interleaved facets—one fixed and one movable. Because these sets have the same area, the efficiency of this beam splitter is nearly unity. The Michelson interferometer uses a Mylar beam splitter (6.3- $\mu\text{m}$  thick in the present case) and has cat's-eye retroreflectors in the interferometer arms. The beam splitter has a maximum efficiency of 0.6 at  $170 \text{ cm}^{-1}$  and an average efficiency over  $50\text{--}200 \text{ cm}^{-1}$  of 0.3.

The far-IR radiation was detected by a germanium bolometer operating at 1.2 K. This type of detector<sup>10</sup> typically has a noise equivalent power of  $5 \times 10^{-13} \text{ W (Hz)}^{-1/2}$  and a responsivity of  $10^4 \text{ V/W}$ . The detector is in a cryostat which also contains the sample under investigation. The overall efficiency<sup>11</sup> of the Fourier systems, including losses in the windows and long pass filter, is estimated to be 0.008 for the Michelson and 0.02 for the lamellar grating.

The laser spectrometer located at Emory University uses a 20-W cw  $\text{CO}_2$  laser to drive a waveguide-type of far-IR cavity. An internal Fabry-Perot interferometer provides line tuning in the cavity, and additional line filtering and wavelength measurement are provided by a second external Fabry-Perot. Some of the far-IR power is introduced into a feedback loop which uses a PZT piezoelectric element to stabilize the  $\text{CO}_2$  laser, although some lines lase with sufficient stability that this feedback is not needed. Further stabilization is provided by a source compensation scheme, where the output of a detector following the sample is electronically divided by the output of a detector preceding the sample to give a ratioed quantity with power fluctuations removed. The two detectors are commercial room-temperature Golay cells with typical responsivities of  $2 \times 10^6 \text{ V/W}$  and noise equivalent powers of  $10^{-10} \text{ W (Hz)}^{-1/2}$ . Standard lock-in amplification of the detector outputs is used with the reference frequency of 11 Hz provided by a mechanical chopper interrupting the far-IR beam. Exact measurements of the laser output power are not available, since there are no well-calibrated far-IR power measuring devices, but estimates based

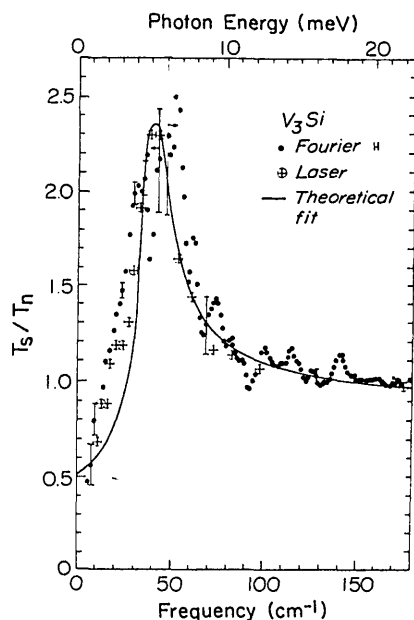


Fig. 1.  $T_s/T_n$  for  $V_3Si$  as measured by the Fourier spectrometers and by the laser system. Fourier points below  $40\text{ cm}^{-1}$  were obtained from the lamellar grating interferometer, while the points above  $45\text{ cm}^{-1}$  were obtained with the Michelson interferometer. Error bars are shown for representative Fourier data points. The circles denoting the laser data have diameters equal to the average laser error bar. A detailed discussion of the theoretical fit is given in Ref. 15.

on the detector sensitivity give typical powers between 0.1 mW and 3 mW for the laser lines. Further details of the laser system have been given elsewhere.<sup>12,13</sup>

The sample was rectangular in shape with dimensions of 7 mm by 15 mm. The  $V_3Si$  film was 20 nm thick, and the substrate was 0.54 mm thick. Both film and substrate were of excellent optical quality. The film front and back surfaces were smooth and highly reflective with no evidence of inhomogeneity or pinholes. The substrate had well-polished parallel faces. Even before the measurements were made, it was obvious that accurate transmission results would be difficult, since an estimate<sup>14</sup> from the dc resistance ( $18.4\ \Omega/\square$ ) showed that the low-temperature transmission would be only about 2%.

The far-IR measurements were made to investigate the superconducting behavior of the sample. For such analysis a useful quantity is  $T_s/T_n$ , the ratio of the sample transmission in the superconducting state to that in the normal state, where both  $T_s$  and  $T_n$  are of the order of a few percent. In the laser and in the Fourier systems the sample state was changed from normal to superconducting by varying the sample temperature. In all measurements the normal state temperature was set at 19 K, but the superconducting temperature varied slightly. It was set at 5.5 K at Emory and at 4.2 K at Ohio State. Since both these values are well removed from the transition temperature (15 K in the present specimen), the temperature difference is not expected to affect our results strongly.

The comparative results for  $T_s/T_n$  between  $6\text{ cm}^{-1}$  and  $180\text{ cm}^{-1}$  are shown in Fig. 1, which also shows a theoretical fit to the data for purposes of comparison. The data are in substantial agreement with theory except for the small features at  $21\text{--}24\text{ cm}^{-1}$  and the low-frequency line shape. The full theoretical analysis is given elsewhere.<sup>15</sup>

The Fourier data were obtained with a resolution of  $1.5\text{ cm}^{-1}$  and an integration time of 4 sec/point. The data shown are from the average of six interferograms in both superconducting and normal states with the lamellar grating and the average of three interferograms in both states with the Michelson. In this latter case, measurements were made up to  $300\text{ cm}^{-1}$ . The intensity maximum was at  $\sim 180\text{ cm}^{-1}$  for the Michelson and at  $24\text{ cm}^{-1}$  for the lamellar grating. These frequencies are determined by a number of factors, including the spectral emittance of the source, the beam-splitter efficiency, and the long pass filter employed.

The Fourier data in Fig. 1 have error bars attached to representative points. These points include those near the intensity maxima, those where the intensity is half of and a quarter of these maxima, and the points where the data change from the lamellar grating to the Michelson (near  $40\text{ cm}^{-1}$ ). The noise levels are calculated as the standard deviations of the individual spectra which were averaged to give the data of Fig. 1. A check on this calculation exists because the sampling interval is about 20% shorter than the maximum allowable value, so the intensity is zero at the high-frequency end of the computed spectrum. The standard deviation of the data in the region gives the noise level, assuming a white-noise spectrum. These two estimates give similar values for the noise level.

For the laser measurements seventeen powerful lines of the many available<sup>13,16</sup> were selected, giving an average frequency spacing of  $\sim 10\text{ cm}^{-1}$  between  $11.2\text{ cm}^{-1}$  and  $175.4\text{ cm}^{-1}$ . Typical lock-in time constants were 0.3 sec. The errors for the laser results, taken as the standard deviations of several measurements, are typically  $\pm 2\%$  of the ratio  $T_s/T_n$ .

The two sets of data can be compared between  $6\text{ cm}^{-1}$  and  $30\text{ cm}^{-1}$  and between  $50\text{ cm}^{-1}$  and  $180\text{ cm}^{-1}$  but not in the peak region  $30\text{--}50\text{ cm}^{-1}$  where the SNR in the Fourier data was quite low. The agreement between laser and Fourier data between  $50\text{ cm}^{-1}$  and  $180\text{ cm}^{-1}$  is excellent, with most of the laser points lying at the means of the oscillations appearing in the Fourier data. The low-frequency agreement is also good except at  $21\text{--}24\text{ cm}^{-1}$ . Here a pronounced shoulder appears in the laser results but not in the Fourier data. The Fourier results do show a slight convexity at the same frequency.

The comparison makes it obvious that there is no serious disparity between results from the older Fourier and the new laser methods. The disagreement at  $21\text{--}24\text{ cm}^{-1}$  may be due to any of several reasons. It may be related to the small difference in superconducting temperatures, which would be of greatest importance at low frequencies. The most intriguing possibility, however, is that the relatively high laser power may cause some nonlinear effect not as yet understood.

Figure 1 clearly shows where each technique has its strengths. The Fourier method in general can give much higher resolution than is available from the quasi-tunable laser. It would probably be practical to double the number of laser lines shown in the figure to give an average spacing of about  $5\text{ cm}^{-1}$ , but a resolution much better than this is unlikely with present techniques. The resolution of the interferometers has been demonstrated to be  $0.1\text{ cm}^{-1}$  for the lamellar grating system<sup>8</sup> and  $0.05\text{ cm}^{-1}$  for the Michelson system.<sup>9</sup> The lowest laser line was at  $11.2\text{ cm}^{-1}$ , whereas the Fourier data extend to  $4\text{ cm}^{-1}$ . At comparable resolution, the random errors in the laser data are equal to those in the Fourier data with the advantage that the former were obtained without cooled detectors requiring costly liquid helium. Further proof of the excellent noise performance of the laser system is given by other measurements<sup>15</sup> in a  $V_3Si$  film of much greater thickness, where the typical transmission is

0.01%. Here the laser spectrometer gave  $T_s/T_n$  with an accuracy only slightly worse than that shown in Fig. 1. The Fourier systems, on the other hand, simply cannot be used with a specimen having this small a transmission.

One feature of the laser system can prove to be either a handicap or an advantage. The narrowness of the laser lines means that interference fringes will appear strongly in cases where the broadband character of the Fourier blackbody source suppresses such effects. A clear advantage of laser spectroscopy is its independence from any computer transformation and analysis of the data and from the related questions of apodization and filtering. On the other hand, the operation of the laser system is at present more complex than that of a Fourier spectrometer. Another measure of the usefulness of the two spectroscopic methods is the actual laboratory time involved in gathering the data shown in the figure. The Fourier results, including setup, data acquisition, and computer data analysis, were obtained in ~20 man hours, while the laser data were obtained in ~60 man hours. While operating, both systems required the attention of one or two researchers.

Our comparisons show that the ideal far-IR-submillimeter spectral source remains elusive. However, the combination of Fourier and laser methods does give the flexibility of choosing the most effective approach for a given spectral measurement problem.

This work was partially supported by NSF grant DMR75-13917 and the Emory University Research Fund.

## References

1. For recent historical reviews of far-IR research, see (a) E. D. Palik, *J. Opt. Soc. Am.* **67**, 857 (1977); (b) N. Ginsburg, *J. Opt. Soc. Am.* **67**, 865 (1977); (c) L. Genzel and K. Sakai, *J. Opt. Soc. Am.* **67**, 871 (1977); (d) P. D. Coleman, *J. Opt. Soc. Am.* **67**, 894 (1977).
2. P. L. Richards, *J. Opt. Soc. Am.* **54**, 1474 (1964).
3. R. C. Hall, D. Vraback, and J. M. Dowling, *Appl. Opt.* **5**, 1147 (1966).
4. C. H. Perry, R. Geick, and E. F. Young, *Appl. Opt.* **5**, 1171 (1966).
5. R. C. Wheeler and J. C. Hill, *J. Opt. Soc. Am.* **56**, 657 (1966).
6. R. Carro and M. Mattoli, *Infrared Phys.* **7**, 25 (1967).
7. I. G. Nolt, R. D. Kirby, C. D. Lytle, and A. J. Sievers, *Appl. Opt.* **8**, 309 (1969).
8. R. L. Henry and D. B. Tanner, *Infrared Phys.*, **19**, 163 (1979).
9. R. B. Sanderson and H. E. Scott, *Appl. Opt.* **10**, 1097 (1971).
10. F. J. Low, *J. Opt. Soc. Am.* **51**, 1300 (1961).
11. B. Carli, D. H. Martin, E. F. Puplett, and J. E. Harries, *J. Opt. Soc. Am.* **67**, 917 (1977).
12. B. L. Bean and S. Perkowitz, *Appl. Opt.* **15**, 2617 (1976).
13. B. L. Bean and S. Perkowitz, *Opt. Lett.* **1**, 202 (1977).
14. R. G. Glover and M. Tinkham, *Phys. Rev.* **108**, 243 (1957).
15. S. W. McKnight, B. L. Bean, and S. Perkowitz, *Phys. Rev. B* **19**, 1437 (1979).
16. J. J. Gallagher M. D. Blue, B. Bean, and S. Perkowitz, *Infrared Phys.* **17**, 43 (1977).

For information regarding the length of a Letter, number of illustrations and tables, and general preparation of manuscripts, see "Information for Contributors" on the eighth page of any issue.

## Testing Coefficients of Circular Objects by Laser Interferometry

G. S. Mikram and N. Vadlam

Pennsylvania State University, Graduate Research Laboratory, University Park, Pennsylvania 16802

Received 10 March 1979

003 6935/79/0000-0000\$01.00

© 1979 Optical Society of America

In a recent article<sup>1</sup> the authors suggested a new type of photographic interferometry where the wave deformation of the object under study is transferred to a plane containing the object for the analysis. The technique was developed for straight cylindrical objects and is extended in this paper on self-centering to the detection of the hump. The purpose of this Letter is to show that laser interferometry can also be utilized for such surfaces if the method simply involves the imaging the object surface on a plane and taking two photographs of the same plane from different locations. The deformation of the surface of the object is captured in the photographs taken, and the height has been developed, they can easily be analyzed using the same method. The discussion analyzing the deformation is given.

A plane surface (labeled  $ABCD$ ) is shown in the fig. The lens holder in the present case is not required for finding double-exposure laser interferograms provided that the image movement between exposures is parallel to the optical axis. Such an interferogram, as shown in Fig. 1, will consist of a diffraction pattern consisting of a set of Young's fringes. These fringes can be seen by placing a translucent screen at the focus position. The angular spacing  $\beta$  of the fringes is given by<sup>2</sup>

$$\sin \beta = \lambda m / D, \quad (1)$$

where  $\lambda$  is wavelength of the light,  $m$  is magnification factor of the photograph, and  $D$  is the surface displacement between the two exposures.

If we take the same exposure from a height of the lens holder with objects of different sizes, then the width of the lens and the support ring will vary but the diameter of the diameter change. Yet all we relate this change in diameter to the final fringes seen in Fig. 1. For this, we must know the distance  $z$  in terms of the object diameter of the object. It is not convenient to find the  $z$  component of  $z$  and needed for the analysis. It is easier to find just how the absolute value  $z = (D^2 + D_0^2)^{1/2}$  at the points of the lens and the support ring.

Figure 1 is a schematic diagram representing the (2) of the plane law of the surface. It is depicting the surface of the object  $OO'$ . The line is fixed at the point  $P$  of the plane surface supporting so that when the radius of the object is  $z$ ,  $OO'$ , the point  $P$  is at the center of  $OO'$ .  $O$  is center of the supporting ring and also that of the coordinate system; and  $y$  directions are parallel to horizontal and vertical, respectively, in the plane of the holder. Point  $R(x, y)$  is a line on the outer supporting ring (fixed) such that a circle on the law of the line  $OO'$  always passes through the point  $P$ .  $\phi$  and  $\theta$  are angles that the lines  $OP$  and  $OR$  make with the  $x$ -axis. With the present holder distance  $OP$  and  $OR$  are equal to the radius  $r$  of the supporting ring.

Suppose we consider point  $G(x, y)$  on the line  $OO'$  such that the distance  $OG = r \cos \phi$  ( $0 \leq \phi \leq \pi$ ). Thus the coordinates of the point  $G$  are the Cartesian

$$x = OG \cos \phi = (r \cos \phi) \cos \phi = r \cos^2 \phi, \quad (2)$$

$$y = OG \sin \phi = (r \sin \phi) \cos \phi = r \sin \phi \cos \phi. \quad (3)$$